Synthesis and properties of new dinuclear organoiron(II) hydrazones combining the potent electron-donating [–(η^5-C$_5$H$_4$)FeCp] fragment with [CpFe(η^6-arene)–]$^+$-type acceptors

Alexander Trujillo [a], Mauricio Fuentealba [a], Carolina Manzur [a], David Carrillo [a,*], Jean-René Hamon [b,*]

[a] *Laboratorio de Química Inorgánica, Instituto de Química, Pontificia Universidad Católica de Valparaíso, Avenida Brasil 2950, Valparaíso, Chile*
[b] *UMR 6509 CNRS-Université de Rennes 1, Institut de Chimie de Rennes, Campus de Beaulieu, F-35042 Rennes Cedex, France*

Abstract

The stereoselective condensation reaction between organometallic hydrazine precursors [CpFe(η^6-p-RC$_6$H$_4$–NHNH$_2$)]$^+$PF$_6^-$ (R = H, (**1**)$^+$PF$_6^-$; Me, (**2**)$^+$PF$_6^-$; MeO, (**3**)$^+$PF$_6^-$; Cl, (**4**)$^+$PF$_6^-$) and (*E*)-(2-ferrocenylvinyl)-methyl ketone, [(*E*)-CpFe(η^5-C$_5$H$_4$)–CH=CH–CO–Me] (**5**), allowed the synthesis of a family of four new push–pull-type homodinuclear hydrazones complexes formulated as (*E*,*E*)-[CpFe(η^6-p-RC$_6$H$_4$)–NHN=CMe–CH=CH–(η^5-C$_5$H$_4$)FeCp]$^+$PF$_6^-$ (R = H, (**6**)$^+$PF$_6^-$; Me, (**7**)$^+$PF$_6^-$; MeO, (**8**)$^+$PF$_6^-$; Cl, (**9**)$^+$PF$_6^-$). These compounds were fully characterized by a combination of elemental analysis and spectroscopic techniques (^{1}H-NMR, IR and UV–Vis), and electrochemical studies in order to prove the π-donor–acceptor interactions between the two metallocenic termini through the asymmetric elongated π-conjugated spacer. Cyclic voltammetry studies reveal an electrochemically reversible one-electron oxidation and an irreversible one-electron reduction step for all the hydrazone derivatives. The redox potentials clearly indicate that the oxidation occurs at the ferrocenyl unit, and the reduction is localized on the mixed sandwich entity. In the electronic absorption spectra, two intense bands are observed in the visible region which undergo positive solvatochromic shifts. The origin of the high-energy absorption band is assumed to be an intraligand charge-transfer (ILCT) transition and the low-energy absorption band is assigned to a metal to ligand charge-transfer (MLCT) transition. Both ILCT and MLCT are shifted to lower energy with increasing spacer length.
© 2003 Elsevier B.V. All rights reserved.

Keywords: Organoiron complexes; Ferrocene complexes; Organometallic hydrazone complexes; Dipolar chromophores; Push–pull complexes

1. Introduction

Over the last few years, there has been considerable interest and, consequently, intensive research efforts devoted to design and develop new highly efficient molecular compounds for optoelectronic applications [1]. This has led to a growing development of organometallic push–pull rod-shaped oligomers that are mainly metallocene-based donor–acceptor materials, and the topic has been the subject of recent reviews [2]. Along this line, we have focused our attention on simple bimetallic model systems [3], made of the robust cationic electron-withdrawing building block [4] [(η^5-Cp)Fe(η^6-arene)–]$^+$ (Cp = C$_5$H$_5$) moiety, linked to the potent donating ferrocenyl unit [–(η^5-C$_5$H$_4$)FeCp], through the asymmetric hydrazonic skeleton spacer, –NH–N=CR– (R = H, Me), in order to investigate the electronic cooperation between both metal centres. Structural, electronic and theoretical (DFT) data have confirmed the ground-state electronic interaction between the two metallocene-based termini for the model compound [CpFe(η^6-C$_6$H$_5$)–NHN=CMe–(η^5-C$_5$H$_4$)-FeCp]$^+$PF$_6^-$ [5].

On the other hand, ferrocenyl chromophores possess some of the largest microscopic and macroscopic second-order nonlinearities reported to date for organometallic compounds [6]. Conventional methods of

---

* Corresponding authors. Tel.: +33-2-23-23-59-58; fax: +33-2-23-23-56-37.
E-mail address: jean-rene.hamon@univ-rennes1.fr (J.-R. Hamon).

enhancing first hyperpolarizability β for donor–acceptor systems include increasing the electron acceptor strength and extending the conjugation pathway. In the pursuit of our previous work, this latter aspect is the focus of the present contribution, in which we describe the preparation and full characterization (IR, ^{1}H-NMR, UV–Vis) of a family of four new Type I non-rod-shaped dipolar chromophores [7] of general formula (E,E)-[CpFe(η^6-p-R-C_6H_4)–NHN=CMe–CH=CH–(η^5-C_5H_4)FeCp]$^+$PF$_6^-$ (R = H, (**6**)$^+$PF$_6^-$; Me, (**7**)$^+$PF$_6^-$; MeO, (**8**)$^+$PF$_6^-$; Cl, (**9**)$^+$PF$_6^-$), where both iron sandwiches are connected by the (E,E)-elongated asymmetric π-conjugated –NH–N=CMe–CH=CH– hydrazonic spacer. Detailed solvatochromic and electrochemical researches have been performed on these organometallic compounds to assess the π-donor–acceptor interactions and the effect of polyenic chain length extension.

2. Results and discussion

2.1. Synthesis and characterization

The preparation of the new organometallic hydrazones (**6**–**9**)$^+$PF$_6^-$ was achieved by reaction of their ionic organometallic hydrazine precursors [CpFe(η^6-p-RC$_6$H$_4$–NHNH$_2$)]$^+$PF$_6^-$ (R = H, (**1**)$^+$PF$_6^-$; Me, (**2**)$^+$PF$_6^-$; MeO, (**3**)$^+$PF$_6^-$; Cl, (**4**)$^+$PF$_6^-$) with one equivalent of the ferrocene-based ketone (E)-[CpFe(η^5-C$_5$H$_4$)–CH=CH–CO–Me] (**5**) in solution containing 10% of hexafluorophosphoric acid, HPF$_6$, as catalyst (Scheme 1). The suspension was refluxed for 7 h under dinitrogen. Complexes (**6**–**9**)$^+$PF$_6^-$ were isolated as air-stable orange solids in moderate yields ranging from 31 to 54%, and they exhibit a good solubility in common polar organic solvents, but are insoluble in diethylether, hydrocarbons and water. The characterization of these four new homodimetallic hydrazones was exhaustively accomplished by elemental analyses and ^{1}H-NMR, IR and UV–Vis spectroscopies (see Section 4 for the details).

The solid IR spectra of complexes (**6**–**9**)$^+$PF$_6^-$ exhibit five major characteristic features: (i) a sharp medium absorption band in the 3345–3337 cm^{-1} region attributed to the ν(N–H) stretching vibration [8]; (ii) a weak band in the 1627–1623 cm^{-1} region assigned to the ν(C=C) stretching mode, (iii) a strong band in the 1562–1555 cm^{-1} region which has been attributed to the stretching mode of the C=N group, (iv) one or two very strong ν(PF$_6$) bands in the 847–831 cm^{-1} region and (v) a strong δ(P–F) band at 558–557 cm^{-1}.

The unique set of signals observed in the ^{1}H-NMR spectra (acetone-d_6, 297 K) clearly indicate that the dinuclear organometallic hydrazones (**6**–**9**)$^+$PF$_6^-$ are stereoselectively formed as the sterically less hindered *trans*-isomer about the N=C double bond. This is in agreement with the previous detailed NMR studies (NOESY and solution dynamics) on the shorter binuclear analogues [CpFe(η^6-C$_6$H$_5$)–NHN=CMe–(η^5-C$_5$H$_4$)FeCp]$^+$PF$_6^-$, and of its crystal structure [5]. For all the compounds, the ethylene bridge signals appear as an AB doublet in the δ 6.49–6.84 ppm range, with a characteristic $^3J_{H-H}$ coupling constant of 16 Hz (see Section 4 for the details) in accordance with the expected *trans* stereochemistry. Both Cp resonances appear as singlets at δ 4.85–4.92 ppm and δ 4.03–4.04 ppm for the cationic and the neutral sandwiches, respectively. The monosubstituted C$_5$H$_5$ ring exhibits a pair of signals at δ 4.23–4.44 ppm, corresponding to the spectrum of an A$_2$B$_2$ system. These signals appear to low field of the C$_5$H$_5$ singlet, showing that all four ring protons are deshielded by the ethendiyl bridge. The upfield-shifted aromatic protons of the coordinated C$_6$-ring (δ 6.04–6.37 ppm) and the deshielded methyl protons of the ferrocenyl-vinyl moiety appeared in their respective expected regions [5]. The low-field position (δ 8.77–9.01 ppm) of the acidic benzylic NH [9] signal may be attributed to the electronic effect of the organometallic moiety [10], and/or its participation in molecular association via intermolecular H-bonding [11].Interestingly, a very good correlation is obtained with ^{1}H-NMR shifts of the benzylic N–H proton resonances (Fig. 1), using the classic Hammett σ_p set of parameters [12] (Eq. (1); R = 0.997). The positive slope indicates that electron-withdrawing substituents induce a marked deshielding of the corresponding ^{1}H-NMR shift. The more the electron-withdrawing the p-R substituent (more positive the σ_p parameter), the more shifted is the NH proton resonance. Those results are well in agreement with earlier literature data for substituted [CpFe(p-X-tolyl)]$^+$PF$_6^-$ derivatives [13].

$$\delta \text{N–H (ppm)} = 0.47\sigma_p + 8.90 \tag{1}$$

2.2. Electronic spectra

The UV–Vis spectral data for the four organodiiron(II) hydrazone complexes (**6**–**9**)$^+$PF$_6^-$ are presented in Table 1 and are consistent with most ferrocenyl chromophores in that they exhibit two charge-transfer bands [14] in the visible region [2,6,17,18]. As in our previous works [5,11] and in agreement with the latest theoretical treatment [19], we assign the lower energy band to a metal to ligand charge-transfer transition (MLCT) and the higher lying absorption as an intraligand π–π^* transition (ILCT). The two CT absorption bands, except the MLCT transition for (**8**)$^+$PF$_6^-$ ($\Delta\lambda_{max} = -12$ nm) [20], exhibit bathochromic shifts on moving from CH$_2$Cl$_2$ ($\varepsilon = 8.90$) to DMSO ($\varepsilon = 47.6$). Analogous solvatochromism has previously been re-
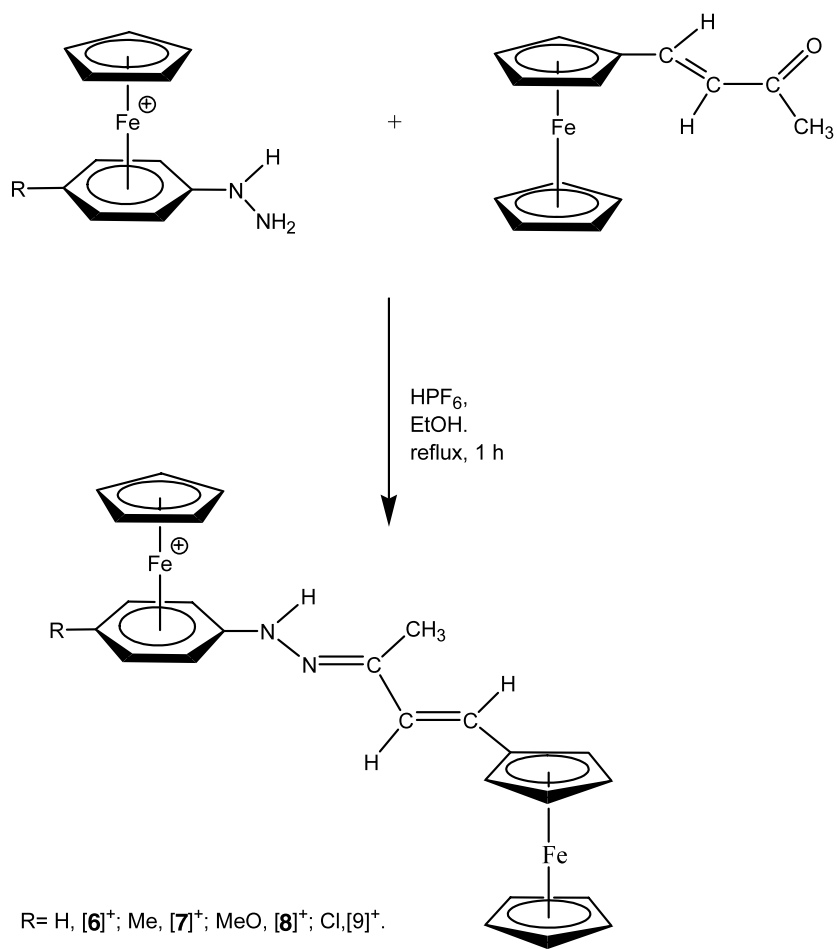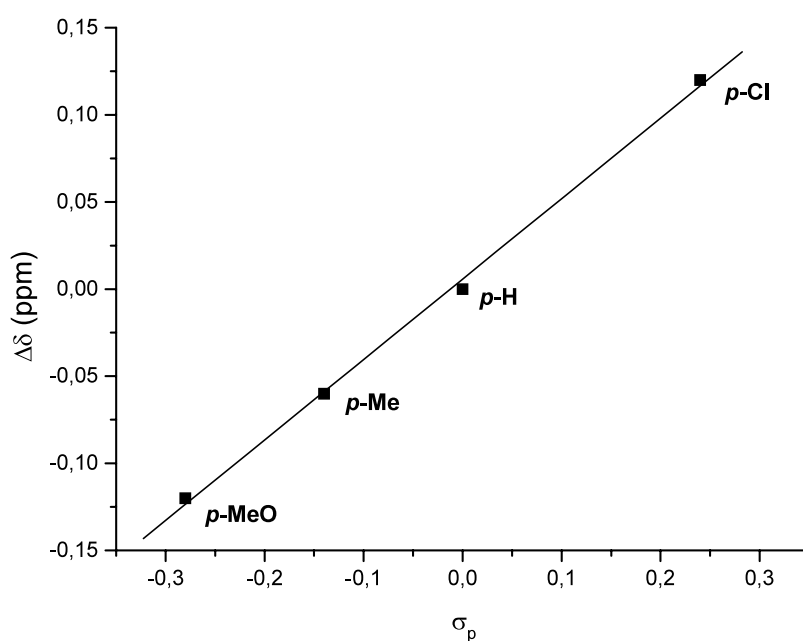
Scheme 1.

Fig. 1. Plot of the N–H ^{1}H-NMR shifts (ppm) vs. σ_p substituent parameters for complexes $(6-9)^+$PF$_6^-$.

Table 1
Electronic and electrochemical data

Compound	UV–Vis (λ_{max} (nm); log ε (L mol^{-1} cm^{-1}))		CV [a] (V vs. Ag | AgCl)	
	CH$_2$Cl$_2$	DMSO	$E_{1/2}$ (ΔE_p (mV)) ferrocene-based [b]	E_{pc} CpFe$^+$ (arene)-based [c]
$(6)^+PF_6^-$	338 (4.03)	354 (3.48)	0.580 (71)	−1.85
	454 (3.53)	456 (2.73)		
$(7)^+PF_6^-$	356 (3.59)	365 (3.78)	0.503 (71)	−1.94
	473 (3.55)	480 (2.72)		
$(8)^+PF_6^-$	320 (4.25)	328 (4.15)	0.511 (73)	−1.88
	480 (3.42)	468 (3.46)		
$(9)^+PF_6^-$	315 (3.56)	336 (4.23)	0.553 (73)	−1.70 [d], −1.88
	475 (3.59)	479 (3.52)		

[a] Recorded in acetonitrile at 298 K with a vitreous carbon working electrode, 0.1 M n-Bu$_4^+$PF$_6^-$ as supporting electrolyte, scan rate 100 mV s^{-1}.
[b] Ferrocene half-wave potential = 0.507 V (79 mV).
[c] Cathodic peak for [CpFe(η^6-C$_6$H$_5$NHNH$_2$)]$^+$PF$_6^-$ = −1.46 V.
[d] See Ref. [23].

ported for a variety of ferrocene donor–acceptor compounds with different types of π-bridges or acceptors [2e,5,6,17,18].

Comparison of the electronic spectra of the two [CpFe(η^6-p-RC$_6$H$_4$)–NHN=CMe–(CH=CH)$_n$–(η^5-C$_5$H$_4$)FeCp] (R = H, Me, MeO; $n = 0$ [5], 1) series clearly demonstrates the influence of the π-bridge length on both bands, as illustrated in Fig. 2 with the p-Me substituted complexes. The absorption bands are red-shifted with increasing the conjugated chain length but the higher energy one (ILCT) moves more rapidly than the lower energy one (MLCT) when R = H and Me, whereas a reverse behaviour is observed with the p-MeO substituent. There is indeed a bathochromic shift of 2363, 4273, 1973 cm^{-1} and 1175, 2060, 2696 cm^{-1} of the ILCT and MLCT bands for R = H, Me, and MeO,
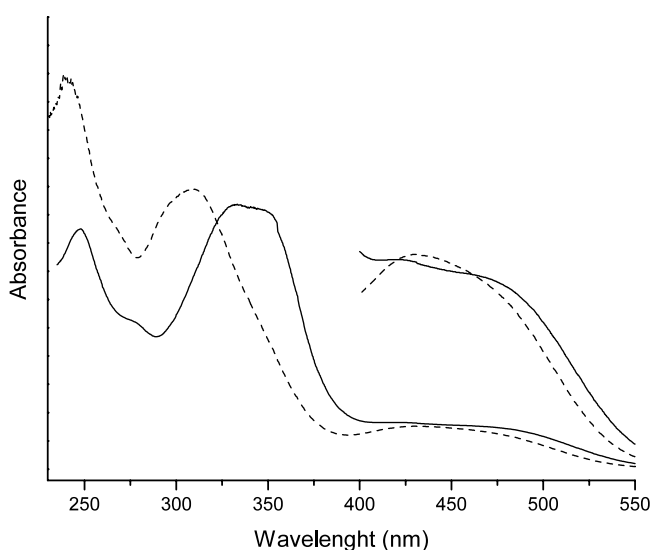

Fig. 2. UV–Vis spectra of (E,E)-[CpFe(η^6-p-MeC$_6$H$_4$)–NHN=CMe–(CH=CH)$_n$–(η^5-C$_5$H$_4$)FeCp]$^+$PF$_6^-$ ($n = 0$, dashed line; $n = 1$, full line) demonstrating the effect of the conjugated bridge on absorption maxima.

respectively. It is noteworthy that these values are of the same magnitude as those reported for many other ferrocenyl series comprising the (E)-(CH=CH)$_n$ bridge [6,17], therefore, justifying the interest of our asymmetric hydrazone spacer in the design of organometallic push–pull materials.

2.3. Electrochemical studies

In order to determine if the elongated conjugated E,E-N=CMe–CH=CH– linker would act as a communication channel between the two metal centers with respect to electrochemical perturbations, we have undertaken the cyclic voltammetry (CV) of the homodimetallic hydrazone complexes $(6–9)^+PF_6^-$. All the compounds were measured in acetonitrile using the same setup, and the acquired electrochemical data are summarized in Table 1. All the complexes display an irreversible reduction step and the chemically reversible ferrocene/ferricinium couple (Fig. 3). The peak to peak separations (ΔE_p) are, however, significantly greater than the ideal value of 60 mV for a fully reversible one-electron process, this probably due to a combination of uncompensated solution resistance and slightly slow electron-transfer kinetics [21a]. However, this difference is similar to that measured for ferrocene under the conditions of the experiment (see Section 4 for details).

Interestingly, the E^0 values of the reversible anodic processes are 73 mV ($(6)^+PF_6^-$) and 46 mV ($(9)^+PF_6^-$) anodically shifted with respect to ferrocene, indicating some degree of electronic interaction between the iron center and the electron-accepting fragment, whereas E^0 are almost identical within the experimental errors for $(7,8)^+PF_6^-$ (Table 1). The amount of the anodic shift depends on both the length of the π-linker and the nature of the donor and acceptor ends [5,6,11,17,18,22]. On the other hand, the four compounds studied undergo
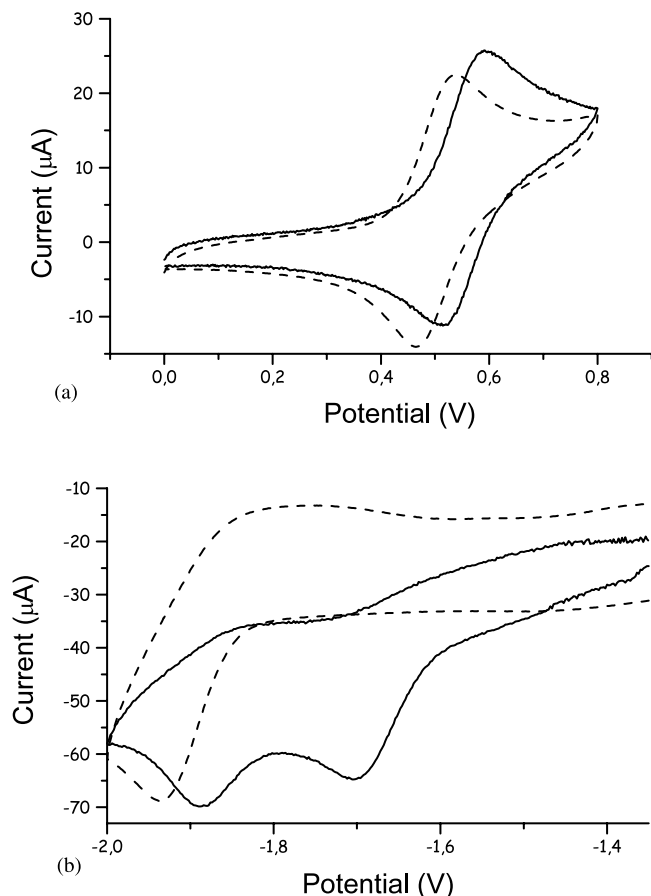
Fig. 3. Cyclic voltammograms of complexes $(\mathbf{7})^{+}PF_{6}^{-}$ (dashed line) and $(\mathbf{9})^{+}PF_{6}^{-}$ (full line): (a) ferrocenyl unit and (b) $[CpFe(p\text{-}RC_{6}H_{4})]^{+}$ fragment; recorded in MeCN/0.1 M $n\text{-}Bu_{4}N^{+}PF_{6}^{-}$ at $T = 293$ K and a voltage sweep rate $v = 0.1$ V s^{-1}.

an irreversible reduction step (Fig. 3b) centered at the mixed sandwich moiety, corresponding to the single-electron reduction of the d^{6}, Fe(II), 18-electron complexes to the unstable d^{7}, Fe(I), 19-electron species [15b,21b]. Note that the cyclovoltammogram of $(\mathbf{9})^{+}PF_{6}^{-}$ exhibits two reduction waves (see Fig. 3b), the more anodic one being attributable to a dechlorination reaction [23]. The very cathodic potential values (Table 1) are very similar to those reported for the monometallic benzaldehyde-hydrazone complexes [9], and are presumably due to the reduction of an in situ generated neutral zwitterionic species [25]. Nevertheless, the electrochemical data make clear that in these binuclear hydrazone complexes, the nature of the HOMO is still dominated by the neutral donating ferrocenyl units, whereas the character of the LUMO is determined by the cationic mixed sandwich, in accordance with the previous experimental and theoretical works [5].

Additionally, and in agreement with the electronic data described above, in comparing the two homobimetallic $-NH-N=C(Me)-(E\text{-}CH=CH)_{n}-$ containing spacer series ($n = 0$ [5], 1), chain lengthening promotes

a significant decrease in the oxidation potential [26] that shifts to less positive direction [6c,6d,6e,6f,6-g,6h,6i,6j,6k,6l,6m,17]. This is probably due to the stabilization of the positive charge of the oxidized species along the π-conjugated chain. This cathodic shift is especially marked for the *p*-Me and *p*-MeO substituted derivatives as observed by the larger decrease of the redox potential than that observed for the parent *p*-H and substituted *p*-Cl counterparts. The mutual donor–acceptor electronic influence would decrease with increasing the distance between the mixed sandwich moiety and the ferrocene moiety, leading to the shift in redox potentials as noted above. These dependencies of the redox potentials on the "polyene" linker length suggest that the two metallocenic termini are electronically communicated significantly via the hydrazone spacer and they behave as a donor–acceptor couple.

3. Concluding remarks

To sum up, we have described an easy access to a homogeneous series of four new organodiiron(II) complexes containing an elongated π-conjugated hydrazonato spacer linking the cationic electron–acceptor mixed sandwich, $[CpFe(\eta^{6}\text{-arene})-]^{+}$, to the neutral electron-donating ferrocenyl group, $[-(\eta^{5}\text{-}C_{5}H_{4})FeCp]$. These homobimetallic compounds can be designed, from a structural point of view, as Type I non-rod-shaped dipolar chromophores [7]. These compounds proved to be electronic conveyors along the conjugated chain, as indicated by the data obtained from the UV–Vis spectra and cyclic voltammetry. Through electronic spectroscopy and electrochemical studies, we have shown that elongation of the unsaturated chain clearly influences the values of the redox potential and the energies of the charge-transfer bands in the electronic spectra. The polarized structure of this type of complexes, which attributes them solvatochromic properties, suggests that they are good candidates for nonlinear optical studies [27]. Work is now directed toward this line.

4. Experimental

4.1. General remarks

All reactions were accomplished using standard Schlenk-line techniques under an atmosphere of dinitrogen. The Schlenk tubes were protected from light to avoid decomplexation of the CpFe^{+} moiety. Solvents were dried and distilled under dinitrogen by standard methods prior to use. Reagents were purchased from commercial sources and used as received. The organometallic hydrazine precursors $[CpFe(\eta^{6}\text{-}p\text{-}$

$RC_6H_5NHNH_2)]^+PF_6^-$ (R = H, (**1**)$^+PF_6^-$; Me, (**2**)$^+PF_6^-$; MeO, (**3**)$^+PF_6^-$; Cl, (**4**)$^+PF_6^-$) were synthesized as previously described [28]. The ferrocene-based ketone (E)-[CpFe(η^5-C$_5$H$_4$)–CH=CH–CO–Me] (**5**) was prepared according to published procedures [29,30]. The elemental analyses were carried out by the Institut de Chimie de Rennes, Microanalysis Service, on a Thermo-FINIGAN Flash EA 1112 CHNS analyser. Solid IR spectra were obtained from KBr disks on a Perkin–Elmer, Model Spectrum One, FT-IR spectrophotometer. Electronic spectra were recorded in CH$_2$Cl$_2$ and DMSO solutions on a Spectronic, Genesys 2, spectrophotometer. The ^{1}H-NMR spectra were recorded on an Avance 400 Digital NMR Bruker spectrometer (400 MHz) at 297 K, and all chemical shifts are quoted in ppm, relative to internal tetramethylsilane (TMS). Cyclic voltammetry experiments were performed at room temperature with a Radiometer PGZ100 potentiostat, using a standard three-electrode setup with a vitreous carbon working and platinum wire auxiliary electrodes and a Ag | AgCl electrode as the reference electrode. Acetonitrile solutions were 1.0 mM in the compound under study and 0.1 M in the supporting electrolyte n-Bu$_4$N$^+$PF$_6^-$ with a voltage scan rate = 100 mV s^{-1}. Under these experimental conditions, the Cp$_2$Fe/Cp$_2$Fe$^+$ couple was located at 0.507 V (ΔE_p = 79 mV). Melting points were determined in evacuated capillaries and were not corrected.

4.2. Preparation of hydrazone complexes

4.2.1. General procedure

In all cases, 0.138 mmol of the ionic organometallic hydrazine, [CpFe(η^6-p-RC$_6$H$_4$NHNH$_2$)]$^+$PF$_6^-$ (R = H, (**1**)$^+$PF$_6^-$; Me, (**2**)$^+$PF$_6^-$; MeO, (**3**)$^+$PF$_6^-$; Cl, (**4**)$^+$PF$_6^-$) were added to 35.0 mg (0.138 mmol) of the ferrocene-based ketone, (E)-{CpFe(η^5-C$_5$H$_4$–CH=CH–CO–Me} (**5**) dissolved in 10 ml of EtOH containing 17.0 µl (0.032 mmol) of 0.81 M HPF$_6$ as the catalyst. The solution was refluxed for 7 h under dinitrogen and allowed first to stand at room temperature and then at −30 °C overnight. The solid precipitated was filtered off and washed with cold EtOH and then with diethyl ether.

4.2.2. (E,E)-[CpFe(η^6-C$_6$H$_5$)–NH–N=CMe–CH=CH–(η^5-C$_5$H$_4$)FeCp]$^+$PF$_6^-$, (**6**)$^+$PF$_6^-$

(**1**)$^+$PF$_6^-$: 51.6 mg. Yield: 54% (46 mg). m.p.: 172 °C (dec). Anal. Calc. for C$_{25}$H$_{25}$F$_6$Fe$_2$N$_2$P (Mr = 610.13 g mol^{-1}): C, 49.21; H, 4.13; N, 4.59. Found: C, 49.45; H, 4.23; N, 4.78%. ^{1}H-NMR (acetone-d_6, δ ppm, TMS): 2.04 (s, 3H, CH$_3$), 4.04 (s, 5H, Cp), 4.25 (s, 2H, C$_5$H$_4$), 4.44 (s, 2H, C$_5$H$_4$), 4.90 (s, 5H, CpFe$^+$), 6.04 (t, 1H, Ar, J_{H-H} = 5.5 Hz), 6.19 (t, 2H, Ar, J_{H-H} = 5.5 Hz), 6.31 (t, 2H, Ar, J_{H-H} = 5.8 Hz), 6.50 (d, 1H, CH, J_{H-H} = 16.1 Hz), 6.81 (d, 1H, CH, J_{H-H} = 16.4 Hz), 8.89 (br s, 1H, NH) ppm. IR (KBr, cm^{-1}): 3342 ν(N–H), 3098 ν(C–H)

arom.; 2963, 2926 ν(C–H) alif.; 1626 ν(C=C), 1556 ν(C=N), 845 and 832 ν(P–F), 558 δ(P–F). UV–Vis (CH$_2$Cl$_2$, λ_{max}, nm (log ε)): 243 (4.18), 276 (3.97), 322 (4.15), 352 (4.15), 393 (3.47), 479 (3.43). (DMSO, λ_{max}, nm (log ε)): 280 (3.91), 331 (4.06), 361 (4.17), 404 (3.03), 456 (3.30).

4.2.3. (E,E)-[CpFe(η^6-p-Me–C$_6$H$_4$)–NH–N=CMe–CH=CH–(η^5-C$_5$H$_4$)FeCp]$^+$PF$_6^-$, (**7**)$^+$PF$_6^-$

(**2**)$^+$PF$_6^-$: 53.5 mg. Yield: 51% (44 mg). m.p. 206 °C (dec). Anal. Calc. for C$_{26}$H$_{27}$F$_6$Fe$_2$N$_2$P (Mr = 624.16 g mol^{-1}): C, 50.03; H, 4.36; N, 4.49%. Found: C, 50.33; H, 4.63; N, 4.55%. ^{1}H-NMR (acetone-d_6, δ ppm, TMS): 2.06 (s, 3H, CH$_3$), 2.34 (s, 3H, Ar–CH$_3$), 4.03 (s, 5H, Cp), 4.24 (t, 2H, C$_5$H$_4$, J_{H-H} = 1.6 Hz), 4.43 (t, 2H, C$_5$H$_4$, J_{H-H} = 1.6 Hz), 4.85 (s, 5H, CpFe$^+$), 6.11 (d, 2H, Ar, J_{H-H} = 5.5 Hz), 6.24 (d, 2H, Ar, J_{H-H} = 5.5 Hz), 6.50 (d, 1H, CH, J_{H-H} = 16.3 Hz), 6.79 (d, 1H, CH, J_{H-H} = 16.3 Hz), 8.83 (br s, 1H, NH). IR (KBr, cm^{-1}): 3345 ν(N–H), 3106 ν(C–H), 2964 and 2925 ν(C–H), 1627 ν(C=C), 1562 ν(C=N), 842 ν(P–F), 558 δ(P–F). UV–Vis (CH$_2$Cl$_2$, λ_{max}, nm (log ε)): 244 (4.30), 278 (4.02), 321 (4.26), 353 (4.22), 398 (3.58), 480 (3.50). (DMSO, λ_{max}, nm (log ε)): 320 (4.07), 353 (4.03), 401 (3.45), 476 (3.46).

4.2.4. (E,E)-[CpFe(η^6-p-MeO–C$_6$H$_4$)–NH–N=CMe–CH=CH–(η^5-C$_5$H$_4$)FeCp]$^+$PF$_6^-$, (**8**)$^+$PF$_6^-$

(**3**)$^+$PF$_6^-$: 55.6 mg. Yield: 47% (41 mg). m.p. 174 °C (dec). Anal. Calc. for C$_{26}$H$_{27}$F$_6$Fe$_2$N$_2$OP (Mr = 640.16 g mol^{-1}): C, 48.78; H, 4.25; N, 4.38. Found: C, 49.18; H, 4.22; N, 4.43%. ^{1}H-NMR (acetone-d_6, δ ppm, TMS): 2.02 (s, 3H, CH$_3$), 3.88 (s, 3H, CH$_3$O), 4.03 (s, 5H, Cp), 4.24 (br s, 2H, C$_5$H$_4$), 4.43 (br s, 2H, C$_5$H$_4$), 4.90 (s, 5H, CpFe$^+$), 6.14 (d, 2H, Ar, J_{H-H} = 5.5 Hz), 6.20 (d, 2H, Ar, J_{H-H} = 5.5 Hz), 6.49 (d, 1H, CH, J_{H-H} = 16.2 Hz), 6.79 (d, 1H, CH, J_{H-H} = 15.4 Hz), 8.77 (br s, 1H, NH). IR (KBr, cm^{-1}): 3338 ν(N–H), 3099 ν(C–H), 2966 and 2924 ν(C–H), 1625 ν(C=C), 1562 ν(C=N), 1248 ν(C–O), 846 and 832 ν(P–F), 558 δ(P–F). UV–Vis (CH$_2$Cl$_2$, λ_{max}, nm (log ε)): 244 (4.30), 279 (3.84), 321 (4.25), 357 (3.92), 390 (3.59), 480 (3.43). (DMSO, λ_{max}, nm (log ε)): 320 (4.07), 353 (4.03), 401 (3.45), 476 (3.46).

4.2.5. (E,E)-[CpFe(η^6-p-Cl–C$_6$H$_4$)–NH–N=CMe–CH=CH–(η^5-C$_5$H$_4$)FeCp]$^+$PF$_6^-$, (**9**)$^+$PF$_6^-$

(**4**)$^+$PF$_6^-$: 56.4 mg. Yield: 31% (27 mg). m.p. 183 °C (dec). Anal. Calc. for C$_{25}$H$_{24}$ClF$_6$Fe$_2$N$_2$P (Mr = 644.58 g mol^{-1}): C, 46.58; H, 3.75; N, 4.35. Found: C, 46.71; H, 3.97; N, 4.61%. ^{1}H-NMR (acetone-d_6, δ ppm, TMS): 2.03 (s, 3H, CH$_3$), 4.03 (s, 5H, Cp), 4.25 (s, 2H, C$_5$H$_4$), 4.43 (s, 2H, C$_5$H$_4$), 4.92 (s, 5H, CpFe$^+$), 6.33–6.66 (m, 5H, C$_6$H$_4$+CH=), 6.84 (d, 1H, CH, J_{H-H} = 16.2 Hz), 9.01 (br s, 1H, NH). IR (KBr, cm^{-1}): 3338 ν(N–H), 3090 ν(C–H) Ar, 2925 and 2856 ν(C–H), 1626 ν(C=C), 1555 ν(C=N), 842 and 833 ν(P–F), 558 δ(P–F). UV–

Vis (CH$_2$Cl$_2$, λ_{max}, nm (log ε)): 245 (4.34), 280 (4.03), 319 (4.18), 353 (4.24), 403 (3.54), 483 (3.57). (DMSO, λ_{max}, nm (log ε)): 264 (4.12), 325 (4.01), 357 (4.27), 402 (3.50), 473 (3.57).

Acknowledgements

References

[1] (a) E. Goovaerts, W.E. Wenseleers, M.H. Garcia, G.H. Cross, Handbook of advanced electronic and photonic materials and devices, in: H.S. Nalwa (Ed.), Nonlinear Optical Materials, vol. 9, Academic Press, New York, 2001, p. 127;
(b) J.J. Wolff, R. Wortmann, in: D. Bethell (Ed.), Advances in Physical Organic Chemistry, vol. 32, Academic Press, New York, 1999, p. 121;
(c) D. Astruc, Electron Transfer and Radical Reactions in Transition-Metal Chemistry, Molecular Electronics, VCH, New York, 1995 (Chapter 4);
(d) S.R. Marder, J.W. Perry, Adv. Mater. 5 (1993) 804;
(e) R.L. Carroll, C.B. Gorman, Angew. Chem. Int. Ed. 41 (2002) 4379;
(f) S. Di Bella, Chem. Soc. Rev. 30 (2001) 355.

[2] (a) J. Heck, S. Dabek, T. Meyer-Friedrichsen, H. Wong, Coord. Chem. Rev. 190–192 (1999) 1217;
(b) I.R. Whittall, M. McDonagh, M.G. Humphrey, Adv. Organomet. Chem. 42 (1998) 291;
(c) N.J. Long, Angew. Chem. Int. Ed. Engl. 34 (1995) 21;
(d) S. Barlow, S.R. Marder, Chem. Commun. (2000) 1555;
(e) J.-P. Launay (Ed.), Molecular Electronics, Gauthier Villars, Paris, New J. Chem. 15 (1991) 97.

[3] C. Manzur, L. Millán, M. Fuentealba, J.-R. Hamon, D. Carrillo, Tetrahedron Lett. 41 (2000) 3615.

[4] (a) H.A. Trujillo, C.M. Casado, D. Astruc, J. Am. Chem. Soc. 121 (1999) 5674;
(b) C. Lambert, W. Gaschler, M. Zabel, R. Matschiner, R. Wortmann, J. Organomet. Chem. 592 (1999) 109;
(c) S. Nakashima, H. Isobe, N. Akiyama, T. Okuda, M. Katada, J. Radioanal. Nucl. Chem. 255 (2003) 287.

[5] C. Manzur, M. Fuentealba, L. Millán, F. Gajardo, D. Carrillo, J.A. Mata, S. Sinbandhit, P. Hamon, J.-R. Hamon, S. Kahlal, J.-Y. Saillard, New J. Chem. 26 (2002) 213.

[6] (a) M.L.H. Green, S.R. Marder, M.E. Thompson, J.A. Bandy, D. Bloor, P.V. Kolinsky, R.J. Jones, Nature 330 (1987) 360;
(b) M. Ahlheim, M. Barzoukas, P.V. Bedworth, M. Blanchard-Desce, A. Fort, Z.-Y. Hu, S.R. Marder, J.W. Perry, C. Runser, M. Staehelin, B. Zysset, Science 271 (1996) 335;
(c) V. Alain, A. Fort, M. Barzoukas, C.-T. Chen, M. Blanchard-Desce, S.R. Marder, J.W. Perry, Inorg. Chim. Acta 242 (1996) 43;

(d) M. Blanchard-Desce, C. Runser, A. Fort, M. Barzoukas, J.-M. Lehn, V. Bloy, V. Alain, Chem. Phys. 199 (1995) 253;
(e) V. Alain, M. Blanchard-Desce, C.-T. Chen, S.R. Marder, A. Fort, M. Barzoukas, Synth. Met. 81 (1996) 133;
(f) J.A. Mata, E. Peris, I. Asselberghs, R. Van-Boxel, A. Persoons, New J. Chem. 25 (2001) 299;
(g) H. Wong, T. Meyer-Friedrichsen, T. Farrell, C. Mecker, J. Heck, Eur. J. Inorg. Chem. (2000) 631;
(h) I. Janowska, J. Zakrzewski, K. Nakatani, J.A. Delaire, M. Palusiak, M. Walak, H. Scholl, J. Organomet. Chem. 675 (2003) 35;
(i) K.N. Jayaprakash, P.C. Ray, I. Matsuoka, M.M. Bhadbhade, V.G. Puranik, P.K. Das, H. Nishihara, A. Sarkar, Organometallics 18 (1999) 3851;
(j) O. Briel, K. Sünkel, I. Krossing, H. Nöth, E. Schmälzlin, K. Meerholz, C. Braüchle, W. Beck, Eur. J. Inorg. Chem. (1999) 483;
(k) J. Mata, S. Uriel, E. Peris, R. Llusar, S. Houbrechts, A. Persoons, J. Organomet. Chem. 562 (1998) 197;
(l) I.S. Lee, S.S. Lee, Y.K. Chung, D. Kim, N.W. Song, Inorg. Chim. Acta 279 (1998) 243;
(m) J.C. Calabrese, L.-T. Cheng, J.C. Green, S.R. Marder, W. Tam, J. Am. Chem. Soc. 113 (1991) 7227.

[7] (a) C. Serbutoviez, C. Bosshard, G. Knöpfle, P. Weiss, P. Prêtre, P. Günter, K. Schenk, E. Solari, G. Chapuis, Chem. Mater. 7 (1995) 1198;
(b) M.S. Wong, U. Meier, F. Pan, V. Gramlich, C. Bosshard, P. Günter, Adv. Mater. 8 (1996) 416.

[8] (a) C. López, R. Bosque, X. Solans, M. Font-Bardia, J. Organomet. Chem. 547 (1997) 309;
(b) C. López, J. Granell, J. Organomet. Chem. 555 (1998) 211.

[9] C. Manzur, L. Millán, W. Figueroa, D. Boys, J.-R. Hamon, D. Carrillo, Organometallics 22 (2003) 153.

[10] D. Astruc, S. Nlate, J. Ruiz, in: D. Astruc (Ed.), Modern Arene Chemistry, Wiley–VCH, Weinheim, 2002, p. 400 (Chapter 12).

[11] C. Manzur, M. Fuentealba, L. Millán, F. Gajardo, M. T. Garland, R. Baggio, J.A. Mata, J.-R. Hamon, D. Carrillo, J. Organomet. Chem. 660 (2002) 71.

[12] (a) J. March, Advanced Organic chemistry: Reactions, Mechanisms and Structures, 4th ed., Wiley, New York, 1992;
(b) C. Hansch, A. Leo, R.W. Taft, Chem. Rev. 91 (1991) 165.

[13] A.N. Nesmeyanov, I.F. Leshchova, Y.A. Ustynyuk, Y.I. Sirotkina, I.N. Bolesova, L.S. Isayeva, N.A. Vol'kenau, J. Organomet. Chem. 22 (1970) 689.

[14] The deconvolution of the two absorption bands give rise to a splitting of both of them into a pair of two independent bands whose λ_{max} are observed in the 319–322 and 352–356 nm, and 390–403 and 479–483 nm ranges for the higher and lower energy transitions, respectively (see Section 4 for details). We also expect d–d transitions, due to both the cationic mixed sandwich [15] and the ferrocenyl unit [16], to be present in the visible part of the spectrum. However, we expect these to be very weak compared to the two charge-transfer transitions.

[15] (a) W.H. Morrison, E.Y. Ho, D.N. Hendrickson, Inorg. Chem. 14 (1975) 500;
(b) J.-R. Hamon, D. Astruc, P. Michaud, J. Am. Chem. Soc. 103 (1981) 758.

[16] (a) Y.S. Sohn, D.N. Hendrickson, H.B. Gray, J. Am. Chem. Soc. 93 (1971) 3603;
(b) Y. Yamaguchi, C. Kutal, Inorg. Chem. 38 (1999) 4861.

[17] (a) J.A. Mata, E. Falomir, R. Llusar, E. Peris, J. Organomet. Chem. 616 (2000) 80;
(b) J.A. Mata, S. Uriel, R. Llusar, E. Peris, Organometallics 19 (2000) 3797;
(c) T. Farrell, T. Meyer-Friedrichsen, M. Malessa, D. Haase, W. Saak, I. Asselberghs, K. Wostyn, K. Clays, A. Persoons, J. Heck, A. R. Manning, J. Chem. Soc. Dalton Trans. (2001) 29;

(d) T. Xie, W.Y. Liu, Y.M. Liang, S.Y. Gao, Polish J. Chem. 75 (2001) 1387;
(e) D.F. Perepichka, I.F. Perepichka, A.F. Popov, M.R. Bryce, A.S. Batsanov, A. Chesney, J.A.K. Howard, N.I. Sokolov, J. Organomet. Chem. 637–639 (2001) 445.

[18] (a) R. Loucif-Saýbi, J.A. Delaire, L. Bonazzola, G. Doisneau, G. Balavoine, T. Fillebeen-Khan, I. Ledoux, G. Puccetti, Chem. Phys. 167 (1992) 369;
(b) A. Houlton, N. Jasim, R.M.G. Roberts, J. Silver, D. Cunningham, P. McArdle, T. Higgins, J. Chem. Soc. Dalton Trans. (1992) 2235;
(c) B.J. Coe, C.J. Jones, J.A. McCleverty, D. Bloor, G. Cross, J. Organnomet. Chem. 464 (1994) 225;
(d) J.S. Schumm, D.L. Pearson, J.M. Tom, Angew. Chem. Int. Ed. Engl. 33 (1994) 1360;
(e) R.P. Hsung, C.E.D. Chidsey, L.R. Sita, Organometallics 14 (1995) 4808;
(f) F. Le Guen, P. Le Poul, B. Caro, R. Pichon, N. Kervarec, J. Organomet. Chem. 626 (2001) 37;
(g) B. Caro, P. Le Poul, F. Robin-Le Guen, J.-Y. Saillard, S. Kahlal, C. Moinet, N. Le Poul, J. Vaissermann, Tetrahedron 58 (2002) 7519;
(h) E. Stankovic, S. Toma, R. Van Boxel, I. Asselbergs, A. Persoons, J. Organomet. Chem. 637–639 (2001) 426.

[19] S. Barlow, H.E. Bunting, C. Ringham, J.C. Green, G.U. Bublitz, S.G.J. Boxer, J.W. Perry, S.R. Marder, J. Am. Chem. Soc. 121 (1999) 3715.

[20] Negative solvatochromism (hypsochromic shift) has already been reported for cationic species such as Fc-pπ-[A]$^+$ (Fc = ferrocenyl, A = acceptor fragment) [6c,6g], since in these species the ground-state dipole moments are opposite in sign to those of the neutral species, due to the acceptor-localized positive charges, but the charge transfer is in the same direction as in the neutral species.

[21] (a) D. Astruc, Electron Transfer and Radical Reactions in Transition-Metal Chemistry, Electrochemistry, VCH, New York, 1995 (Chapter 2);
(b) D. Astruc, Electron Transfer and Radical Reactions in Transition-Metal Chemistry, Electrochemistry, VCH, New York, 1995, p. 147 (Chapter 2).

[22] (a) Minor [17e]or no [22b] anodic shift with increasing the number or strength of electron-withdrawing substituents on the acceptor moiety has recently been observed.;
(b) P. Zanello, G. Opromolla, F. Fabrizi de Biani, A. Ceccanti, G. Giorgi, Inorg. Chim. Acta 255 (1997) 47.

[23] This fully irreversible wave could be attributed to the 2-electron reduction of the C−Cl functionality, following the ECE mechanism for the reduction of Ar−X into Ar$^-$ and X$^-$ [24]. Its integrated area is twice that of the wave at −1.88 V, ascribed to the in situ generated (**6**)$^+$PF$_6^-$.

[24] D. G. Peters, Organic electrochemistry, in: H. Lund, O. Hammerich (Eds.), Halogenated Organic Compounds, 4th ed., Marcel Dekker, New York, 2001, p. 341 (Chapter 8).

[25] The benzylic N−H group is indeed strongly activated by both the electron-withdrawing organometallic moiety CpFe$^+$ and the imine functionality. Therefore, the thermally stable zwitterion [CpFe$^+$(p-RC$_6$H$_4$)N$^-$−N=CMe−(C$_5$H$_4$)FeCp] can be easily formed by deprotonation in the electrochemical medium. Contrary to their shorter congeners (without the −CH=CH− unit [5]), all attempts to characterize the non-deprotonated compounds (**6**−**9**)$^+$PF$_6^-$ by CV failed, whatever the experimental conditions used (solvent, nature of the electrodes).

[26] The redox potentials of compounds (**6**–**9**)$^+$PF$_6^-$ and those of their counterparts prepared in Ref. [5] are compared relative to the ferrocene/ferricinium couple used in both cases as internal reference.

[27] I.D.L. Albert, T.J. Marks, M.A. Ratner, J. Am. Chem. Soc. 120 (1998) 11174.

[28] C. Manzur, E. Baeza, L. Millán, M. Fuentealba, P. Hamon, J.-R. Hamon, D. Boys, D. Carrillo, J. Organomet. Chem. 608 (2000) 126.

[29] D. Prim, A. Auffrant, Z.F. Plyta, J.-P. Tranchier, F. Rose-Munch, E. Rose, J. Organomet. Chem. 624 (2001) 124.

[30] Under the electrochemical conditions used here, the half-wave potential of the ferrocenyl moieties for the ketone derivatives (**5**) ($E_{1/2} = 0.58$ V, $\Delta E_p = 85$ mV) is more anodic than that measured for ferrocene, meaning some degree of electronic interaction between the iron center and the electron-accepting ketone fragment.